PNC TN941 76－104

Local Boiling of Sodium in Downstream of Local Flow Blockage in a Simulated LMFBR Fuel Subassembly

September, 1976

POWER REACTOR AND NUCLEAR FUEL DEVELOPMENT CORPORATION

動力炉・核燃料開発事業団 (Power Reactor and Nuclear Fuel Development Corporation)

Paper to be presented at the International Meeting on Fast Reactor Safety and Related Physics, October 5-8, 1976, Chicago, Illinois.

LOCAL BOILING OF SODIUM IN DOWNSTREAM OF LOCAL FLOW BLOCKAGE IN A SIMULATED LMFBR FUEL SUBASSEMBLY

Y. Kikuchi, Y. Daigo and A. Ohtsubo

Power Reactor and Nuclear Fuel Development Corporation
O-arai, Ibaraki, Japan

ABSTRACT

This paper deals with local sodium boiling in the downstream of a six-subchannel blockage in an electrically heated LMFBR fuel subassembly mockup.

The first series of experiments were conducted to measure temperature distributions in the downstream of the blockage under non-boiling conditions. The measured temperature rise due to the blockage agreed fairly well with the calculation by the LOCK code. When the experimental results are extrapolated to reactor conditions, the temperature rise due to the six-subchannel blockage is estimated to be less than 250°C.

The second series of experiments were performed to investigate local boiling phenomena. In the local boiling region, no flow instability was observed since the subchannels near the wrapper wall were still filled with subcooled liquid. In the nearly bulk boiling region, however, considerable upstream voiding occurred and then the inlet flow was reduced, leading to final dryout.

The boiling caused a considerable increase in acoustic noise intensity. The root-mean-square (RMS) noise level of approximately 20 mbar obtained in the present local boiling experiments with sodium is much higher than that (approximately 0.5 mbar) in the ordinary nucleate boiling experiments with water. The peak observed in the hertz ranges was due to the repetition of bubble formation and collapse. In the kilohertz ranges, however, resonance peaks were superposed on a smooth curve with a broad peak at approximately 7 kHz.

The boiling caused a considerable increase in outlet flow fluctuation. The maximum RMS value of the fluctuation was 1.33 m/s. The peak observed in the hertz ranges was again due to the repetition of bubble formation and collapse.

The frequency (2.9 s^{-1} and 20.2 s^{-1}) of bubble formation decreased with the increase of the bubble size at its point of maximum development. The product of the bubble frequency and the equivalent diameter was found to be constant.

INTRODUCTION

Anomalous sodium boiling caused in some accidents is an important problem for safety considerations in the liquid metal cooled fast breeder reactor (LMFBR), since sodium boiling might lead to fuel failure propagation, and finally total core disruption. Experimental studies have been carried out in this connection, using the Sodium Boiling and Fuel Failure Propagation Test Loops, SIENA installed at the O-arai Engineering Center, Power Reactor and Nuclear Fuel Development Corporation.

In the earlier bulk boiling experiments under loss-of-flow conditions[1], it was revealed that the voiding pattern observed in the single-pin geometry agreed fairly well with the calculation by the NAIS-P2 code (single-bubble slug-ejection model), whereas in the seven-pin geometry, two-dimensional voiding patterns were dominant. No significant effects were observed of the temperature ramp rate on the incipient-boiling (IB) wall superheat. The pressure rise at the initial vaporization compared well with the vapor pressure corresponding to the IB wall superheat. The pressure pulse occurring at the vapor collapse correlated reasonably

well with the re-entry velocity of the liquid column and agreed well with the prediction by sodium hammer analysis. The residual liquid film thickness (0.05 mm and 0.45 mm) became thinner with higher IB wall superheat.

In the single pin forced convection boiling experiments[2], however, the observed two-phase flow pattern was in the sequence of bubbly flow, slug flow and annular (mist) flow in sodium as in the case of water. The spectra of acoustic noise emitted with boiling did not differ distinctly from that registered when boiling was not apparent. When the noise was filtered to eliminate its low-frequency components, the noise intensity level associated with boiling first increased sharply with rising heat flux to attain a maximum value, then decreased somewhat and remained constant thereafter. The frequency (3.9 s^{-1} and 9.3 s^{-1}) of bubble formation decreased with increasing bubble size at its point of maximum development. The product of the bubble frequency and the equivalent diameter with the value of 77.8 mm/s (=280 m/h) stayed relatively constant as suggested by Jakob[3] for pool boiling with water.

The present experiments have been conducted to investigate local sodium boiling in the downstream of a local flow blockage in a seven-pin bundle. This paper gives the experimental results of local boiling phenomena, with particular emphasis on the behavior of two-phase flow pattern, the characteristics of boiling acoustic noise and outlet flow fluctuation and the frequency of bubble formation. In addition, the experimental results of temperature distributions in the downstream of the blockage under non-boiling conditions will be compared with the calculation by the computer code LOCK.[4]

EXPERIMENTAL EQUIPMENT AND OPERATING PROCEDURES

Loop

A series of experiments were carried out in the Sodium Boiling and Fuel Failure Propagation Test Loops, SIENA at PNC's O-arai Engineering Center. The details of the SIENA loops are described in reference 1. Only a brief recapitulation will be given here.

The SIENA loops have three test sections: T-1, for single-pin experiments; T-2, for 7-pin experiments; and T-3, for 19-pin or 37-pin experiments. The main circulation pump can provide sodium flow up to 5×10^{-3} m^3/s. The maximum power of 650 kW can be supplied to the electrically heated pins.

Test Section

Figure 1 shows a sketch of the locally blocked test section. In order to simulate an LMFBR fuel subassembly, an electrically heated seven-pin bundle was centered in a hexagonal tube, 24 mm flat-to-flat distance inside. The heater pins, which were specially made for the present study by Sukegawa Electric Co., Ltd., were 6.5 mm in diameter and approximately half as long as the fuel pins of the Japanese prototype LMFBR, MONJU. The heater pins can be operated at the maximum heat flux of 300 W/cm^2 in the flowing sodium of 900°C. The pitch-to-diameter ratio (P/D) was 1.22. At the distance of 350 mm from the start of the heated section the six central subchannels were blocked by a 0.5 mm thick stainless steel plate welded on the upstream side of a grid spacer. The grid spacer, which consisted of seven stainless steel tubes of 7.9 mm in outer diameter and 5 mm in height, was specially made for the present study. The blockage and the grid spacer covered 42 % of the total flow area.

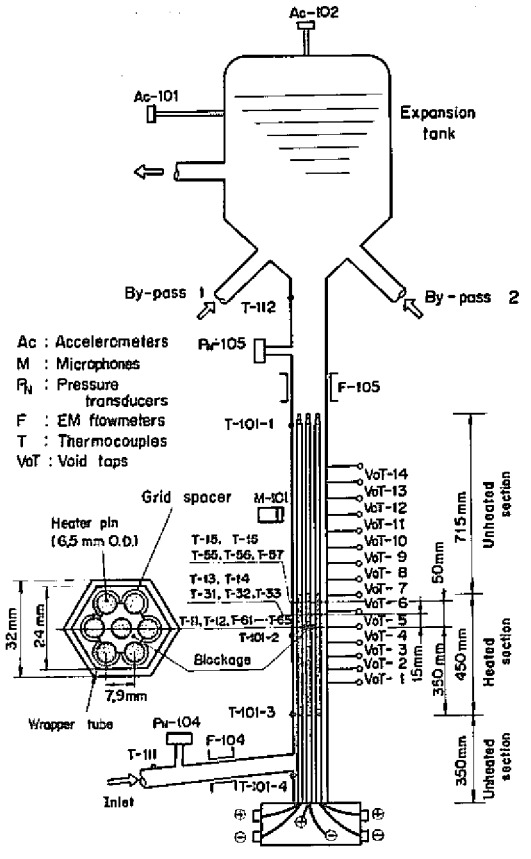

Fig. 1 Locally blocked seven-pin bundle

A compensating heater and a thermal insulator were equipped on the outer wall of the hexagonal tube to compensate heat dissipation from the wall and to keep the outer wall in an adiabatic condition. The by-pass of the test section simulated other subassembly channels adjacent to the boiling subassembly.

The pin surface temperatures (T-11, through T-65) were measured by many chromel-almel thermocouples of 0.3 mm in diameter, which were embedded in the outer surface of each pin. Their hot junctions were located at the axial locations: 0 mm, 15 mm and 50 mm downstream from the blockage. Thermocouples T-101-1, through T-101-4 were welded on the outside surface of the hexagonal tube to measure the local tube temperatures. The inlet and outlet temperatures were measured by the thermocouples T-111 and T-112, respectively.

Potential-tap type void meters (VoT-1, through VoT-14) were used for detecting the formation of vapor bubbles at boiling inception and their subsequent behavior. The sodium velocities at the inlet and outlet were measured by the electromagnetic flowmeters F-104 and F-105, respectively.

Three types of acoustic transducers were used in order to measure the boiling acoustic noises. The first were accelerometers Ac-101 and Ac-102 —— Kistler Model 815A5 —— mounted onto waveguides which were placed to the expansion tank. Secondly strain-gauge type pressure transducers P_N-104 and P_N-105 —— Shinkoh Model PR-5S and PR-10S —— were provided at the inlet and outlet of the test section to measure the pressure changes in boiling sodium. The third was a condenser type microphone M-101 —— Sony Model ECM-21 —— which was set outside the test section.

All the signals from these instruments were recorded by analog data recorders as well as by a digital data acquistion system.

Operating Procedure

The experiments were performed in the following manner. The oxygen concentration in sodium was controlled down to 10 ppm with a purification system. All the instruments were calibrated before the experiments and checked periodically during experiments.

In the first series of experiments, where temperature distributions were measured in the downstream of the blockage under non-boiling conditions, the flow rate was set and the heater pins were adjusted to a fixed power level. Sufficient time was allowed for the test section to reach steady-state conditions prior to experiments. To verify the consistency of the data, several runs were repeated.

The non-boiling experiments were conducted under the following conditions:

Flow velocity	$0.27 \sim 5.00$ m/s
Inlet temperature	$261.5 \sim 374.6$°C
Heat flux	$3.8 \sim 63.1$ W/cm^2.

In the second series of experiments, however, where local boiling phenomena were investigated, the inlet temperature and flow rate were held constant and the heat flux was gradually increased up to boiling inception. After boiling had thus set in, the heat flux was further increased step by step until dryout occurred as it was confirmed that the test section had not failed even under the final dryout condition.

The boiling experiments were conducted under the following conditions:

Flow velocity	$0.40 \sim 2.52$ m/s
Inlet temperature	$463 \sim 537$ °C
Heat flux	$54.2 \sim 270.1$ W/cm^2
Cover gas pressure	$1.03 \sim 1.05$ bars.

RESULTS AND DISCUSSIONS

Temperature Distributions in the Downstream of the Blockage under Non-Boiling Conditions

Figure 2 shows a typical measured longitudinal pin surface temperature distribution in the downstream of the blockage under a non-boiling condition. The experimental results were compared with the analytical results calculated by the LOCK code, whose description is given in reference 4. In this figure the horizontal axis X is the distance from the blockage, and the vertical axis $T-T_{B(X=0)}$ is the temperature difference between the pin surface temperature and the bulk coolant temperature at the blockage section. It can be seen from the figure that the temperature attains a local peak on the surface of the central pin at the blockage (X=0 mm) and decreases with the distance from the blockage. The temperature rise also occurs on the surface of an outer pin facing the hexagonal tube. This may be attributed to the heat resistance effect of the grid spacer covering the outer pin surface.

Calculations by the LOCK code were performed for the same conditions: flow

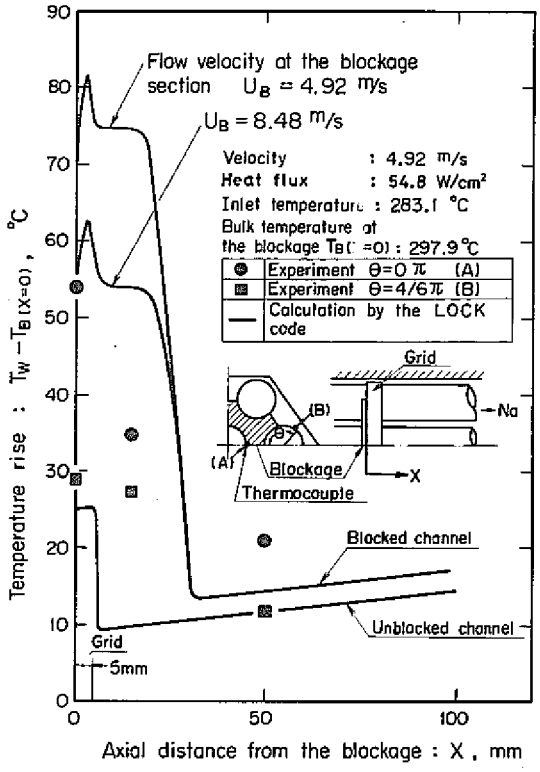

Fig. 2 Comparison of axial pin surface temperature distribution in the downstream of the blockage observed in the experiment with that calculated by the LOCK code

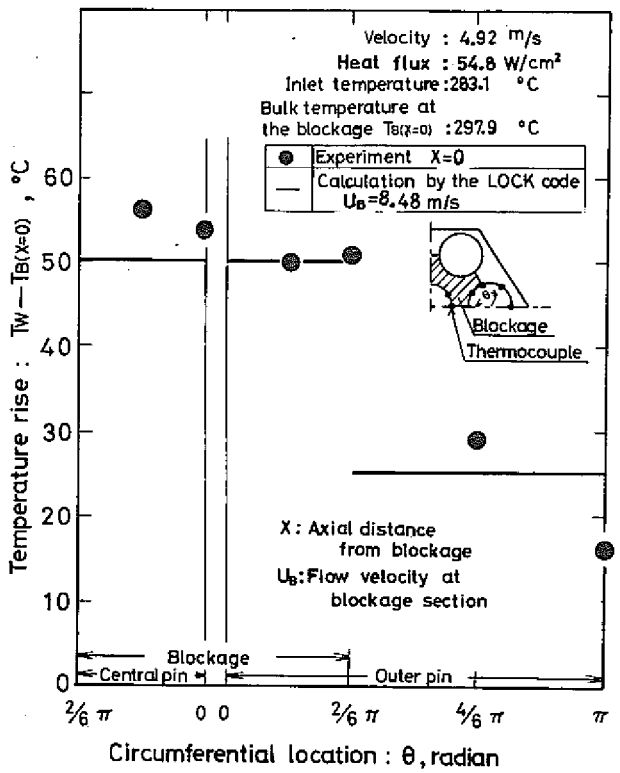

Fig. 3 Comparison of circumferential pin surface temperature distribution at the blockage section observed in the experiment with that calculated by the LOCK code

velocity, 4.92 m/s (at the normal cross section); heat flux, 54.8 W/cm^2; and inlet temperature, 297.9°C. The parameter U_B is the flow velocity in outer subchannels at the blockage section. U_B=4.92 m/s corresponds to zero increase in flow velocity, and U_B=8.48 m/s is the flow velocity, with the increase of flow velocity at the blockage section taken into account. The calculated curve for U_B=8.48 m/s agrees fairly well with the measured temperature rise due to the blockage.

Figure 3 shows the measured circumferential pin surface temperature distribution at the blockage section. The experimental results were again compared with the LOCK code calculation. The thermocouple arrangement to measure the temperature of each pin surface is shown in Fig. 3. The experimental conditions were: flow velocity, 4.92 m/s; heat flux, 54.8 W/cm^2; and inlet temperature, 297.9°C. This figure shows that the temperature is nearly constant in the blocked region (between 0 and 2/6 π) and decreases steeply in the unblocked region (between 2/6 π and π). The calculation was conducted for U_B=8.48 m/s and agrees well with the measured temperature distribution at the blockage section.

If the experimental results are extrapolated to the prototype reactor conditions, in which the heat flux is 200 W/cm^2 and the flow velocity is 5 m/s, the temperature rise due to the central six-subchannel blockage is estimated to be less than 250°C. In the estimation by LOCK no increase in flow velocity is assumed at the blockage section, i.e. U_B is taken as 5 m/s in spite of a little increase in flow velocity at the blockage section in the fuel subassembly.

Two-Phase Flow Pattern

Incipient Boiling and Bubbly Flow

Figure 4(a) represents typical patterns of inlet and outlet flow velocities, inlet and outlet temperatures, pin surface temperatures, void fractions, and inlet and outlet pressure rises during the incipient boiling and bubbly flow regimes. The experimental conditions were: inlet temperature, 502°C; the inlet flow velocity, 0.96 m/s; and cover gas pressure, 1.05 bars.

As can been seen in the figure, the outlet flowmeter F-105 registers an abrupt change upon boiling inception followed by oscillations. These oscillations indicate a repetition of bubble

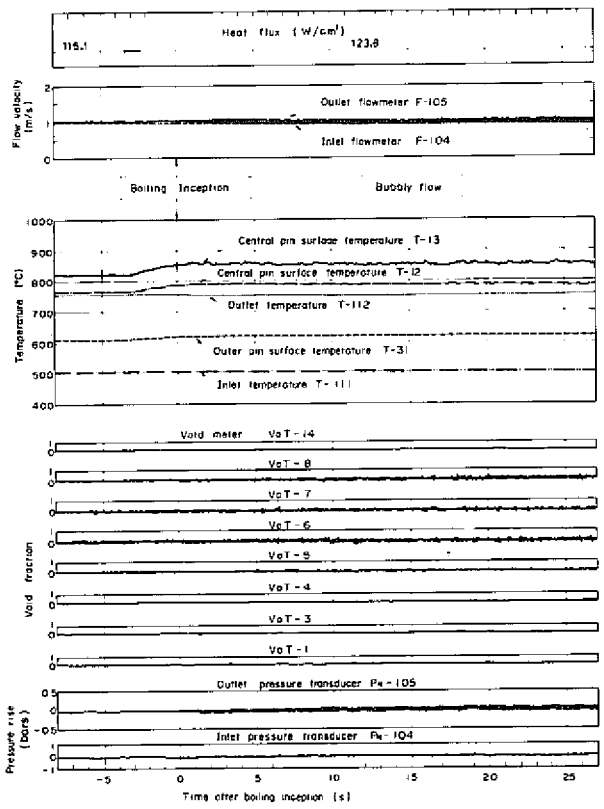

(a) Incipient boiling and bubbly flow

formation and collapse at a fixed frequency. But the inlet flow rate remains constant, as confirmed by the record of F-104.

On the other hand, the center pin surface temperature T-13, which is close to the boiling region, fluctuates after boiling inception. The other temperatures T-12 and T-31 indicate no fluctuations, these thermocouples being located out of the region influenced by boiling. It is clear from the outlet temperature (T-112) that the liquid around the vapor bubbles is highly subcooled. When the tip of the bubble enters the subcooled liquid, its growth is markedly inhibited. Thus, the void meters cannot detect incipient boiling since they send no output signals before a considerable amount of bubbles has accumulated.

The inlet and outlet pressure transducers (P_N-104 and P_N-105, respectively) indicate oscillations due to a

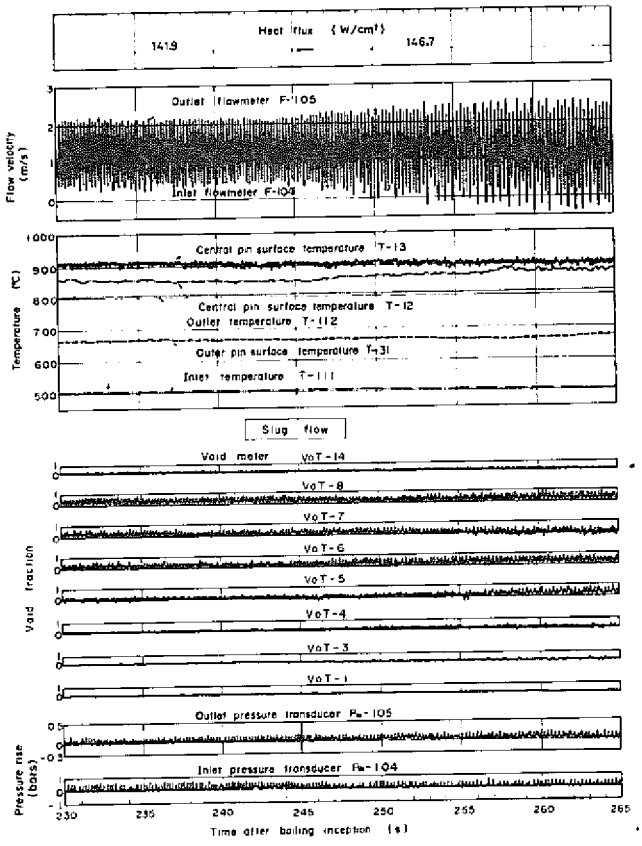

(b) Slug flow

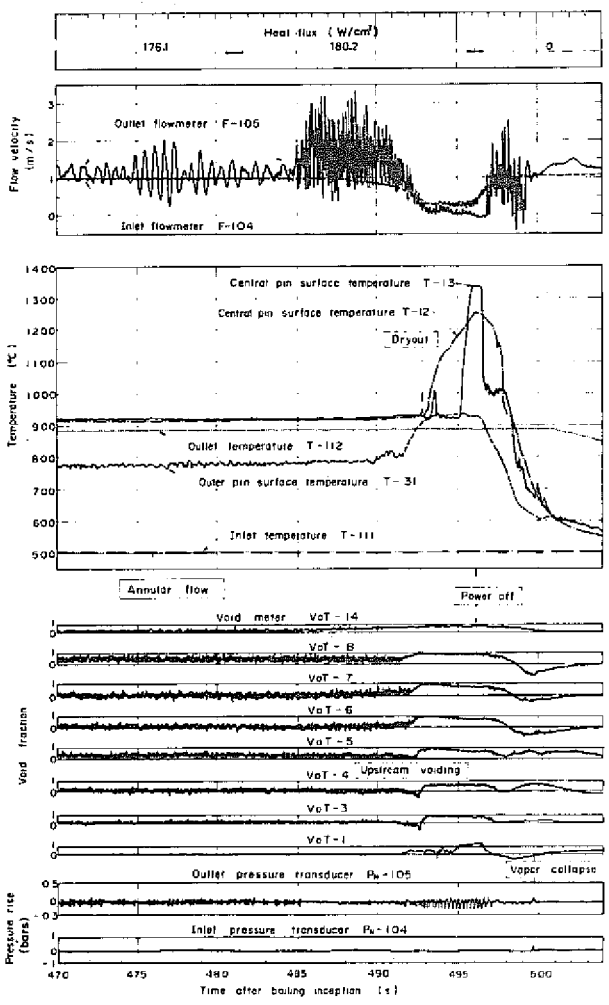

(c) Annular flow and dryout

Fig. 4 Records of signals from flowmeters, thermocouples, void meters and pressure transducers during steady-state boiling in a locally blocked seven-pin bundle —— run No. 7(6)LB-214

repetition of bubble formation and collapse after boiling inception.

Slug Flow Figure 4(b) shows the changes in the heat flux, flow velocities, temperatures, void fractions and pressure rises after the establishment of a slug flow. It is to be noted that violent oscillations are recorded for the outlet flow velocity (F-105), the void fractions (VoT-6, VoT-7 and VoT-8), and the inlet and outlet pressure rises (P_N-104 and P_N-105 respectively), while the inlet flow velocity (F-104) remains at a nearly constant value. These violent oscillations indicate that bubbles, which repeatedly form and collapse, are larger in this regime than in the bubbly flow regime.

The pin surface temperature (T-13) fluctuates and attains the saturation temperature of sodium. The other temperatures, except the inlet temperature T-111, rise with increasing heat flux, but these temperatures are still below saturation, and the boiling continues in a subcooled environment.

Annular Flow and Dryout Figure 4(c) shows the changes in the heat flux, flow velocities, temperatures, void fractions and pressure rises under annular flow and dryout conditions. In the first half of this period covered, the violent oscillations in the outlet flow rate (F-105) established during slug flow settle down to a wavy pattern of a fairly long period. This change is brought about by the bubble collapse being slowed down, since the outlet temperature (T-112) is nearly at the saturation temperature of sodium, which begins bulk boiling. The foregoing behavior indicates an annular flow (or annular mist flow) regime, in which saturated sodium vapor or vapor mixed with liquid sodium globules flows between films of liquid sodium flowing along the wall surface. During this period the pressure are lower than in the slug flow regime, in particular, no signals appear in the inlet pressure transducer, P_N-104. The decreasing pressures can be attributed to the two factors: firstly the subcooling decrease slows down the bubble collapse rate and hence reduces the pressure source, and secondly the large amount of vapor increases the pressure absorption.

A further increase of the heat flux up to 180.2 W/cm^2 produces an alternate mode in the outlet flow signals from F-105. This change is due to the ejection of liquid films and/or liquid globules, then to the succeeding generation of a large amount of vapor bubbles. This succeeding generation of vapor then suppresses the inlet flow rate, as revealed by the sharp valley in the record of F-104. The rapid upstream voiding occurs, which is indicated by the rapid increase of void fractions. A ripple pattern is superposed on the void-meter signals. This ripple pattern, which is similar to those in the outlet flow velocity (F-105) and the outlet pressure (P_N-105), occurs at the time when the disturbance waves of the liquid film on the wall surface travel rapidly in the annular mist flow. In this period the pin surface temperatures (T-12 and T-13) register a sharp rise, which implies the occurrence of dryout of the residual liquid film. The heater pins being exposed to the danger of burnout, the input power to the heater pins was quickly shut off. The pin surface temperatures, however, decrease slowly due to the heat capacity of the heater pins.

Boiling Acoustic Noise

Among the various methods proposed for early detection of local sodium boiling, the measurement of acoustic noise signals associated with boiling phenomena appears to be most promising.

Instrumentation System Three types of acoustic transducers were used in the present experiments, as described in the section on the experimental equipment. The signals from these acoustic transducers were then amplified and recorded on an Ampex Model FR-1800L tape recorder. The tape recordings of the acoustic signals were analyzed using an EMR Model 1510 real-time analyzer. An NF Circuit Model M-172TA AC voltmeter was used for measuring the acoustic noise intensity, regulated by a Multimetrics Model AF-120 filter.

Acoustic Noise Intensity Figure 5 shows the effect of changes in heat flux q on the intensity ratio I/I_o measured by the pressure transducer P_N-105 during a typical boiling run 7(6)LB-214, where I is the noise intensity at a given heat flux q, and I_o the noise intensity in the absence of boiling. It is seen that the acoustic noise intensity first increases with the rise in the heat flux, and after attaining a maximum, decreases somewhat to remain more or less constant thereafter. This tendency is similar to the previous single-pin experiments[2].

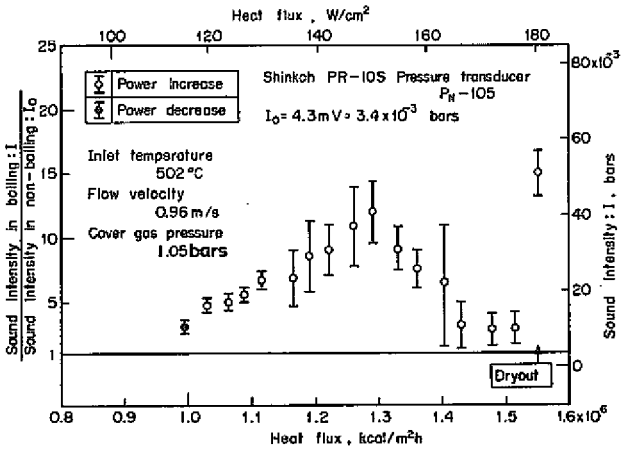

Fig. 5 Effect of heat flux on intensity of acoustic noise with boiling in a locally blocked seven-pin bundle —— steady-state boiling run 7(6)LB-214

At the final rapid upstream voiding which resulted in dryout, however, the acoustic intensity again increases sharply.

During the first stage of boiling, preceding the attainment of maximum noise intensity, the boiling is considered to be in a state of developing nucleate boiling (mainly bubbly and slug flows). In this state the acoustic noise caused by the collapsing bubbles increases with rising heat flux since the liquid around the bubbles is yet so highly subcooled that the bubbles collapse completely although the bubbles become larger with higher heat flux.

Fully developed boiling may be established after the point of maximum noise intensity. The decreasing noise intensity can be attributed to the two factors. The first is the decrease in subcooling, which slows down the bubble collapse and so reduces the noise source. Secondly, the increased amount of vapor in the channel increases the acoustic absorption.

The final noise increase resulting from the rapid upstream voiding is due to the liquid globules and/or liquid films travelling rapidly in the annular mist flow and colliding with the downstream liquid pool.

A similar effect of heat flux on the acoustic noise intensity was measured by the other acoustic transducers.

The acoustic noise intensity (approximately 20 mbar in the RMS value) in the present local boiling of sodium is much higher than that (approximately 0.5 mbar) obtained in the ordinary pool boiling in water[5]. The above observation indicates that the measurement of acoustic noise signals associated with sodium boiling phenomena is promising for early detection of local sodium boiling in LMFBR fuel subassemblies.

Spectrum of Acoustic Noise Figure 6(a) shows the frequency spectra of acoustic noises measured by the pressure transducer P_N-105 during the boiling run 7(6)LB-214. It can be seen that the boiling causes a considerable increase in intensity at all frequencies. The peak observed at the frequency of 19.6 Hz for the heat flux of 120.0 W/cm^2, is due to the repetition of bubble formation and collapse. The peak at 4.4 Hz for 146.7 W/cm^2 is also due to the same repetition.

Figure 6(b) shows the frequency spectra of acoustic noises measured by the accelerometer A_c-102 during the same boiling run 7(6)LB-214. The frequency range in this figure is higher than that in the former Fig. 6(a). The boiling causes a considerable increase in intensity at all frequencies, but the frequency spectra do not change markedly during boiling, from boiling inception until dryout. Resonance peaks are superposed on a smooth curve with a broad peak at approximately 7 kHz for all the measurements.

Outlet Flow Fluctuation with Boiling

The boiling causes an increase in outlet flow fluctuations, as shown in the former Fig. 4. From this fact the measurement of outlet flow fluctuation signals with boiling appears to be promising for the early detection of local boiling.

Intensity of Flow Fluctuation

Figure 7 shows the effect of the heat flux on the intensity of outlet flow velocity fluctuation during the boiling run 7(6)LB-214. In this figure the fluctuation intensity is expressed in root-mean-square values. It is seen that the fluctuation intensity first increases with rising heat fluxes, and after attaining a maximum (1.33 m/s), then decreases. Upon the final rapid upstream voiding which resulted in dryout, however, the fluctuation intensity again increases sharply. The heat flux effect shown in this figure is similar to that already shown in Fig. 5.

During the first stage, preceding the attainment of maximum fluctuation intensity, the boiling is considered to be in a state of developing nucleate boiling and no bubbles reach the posi-

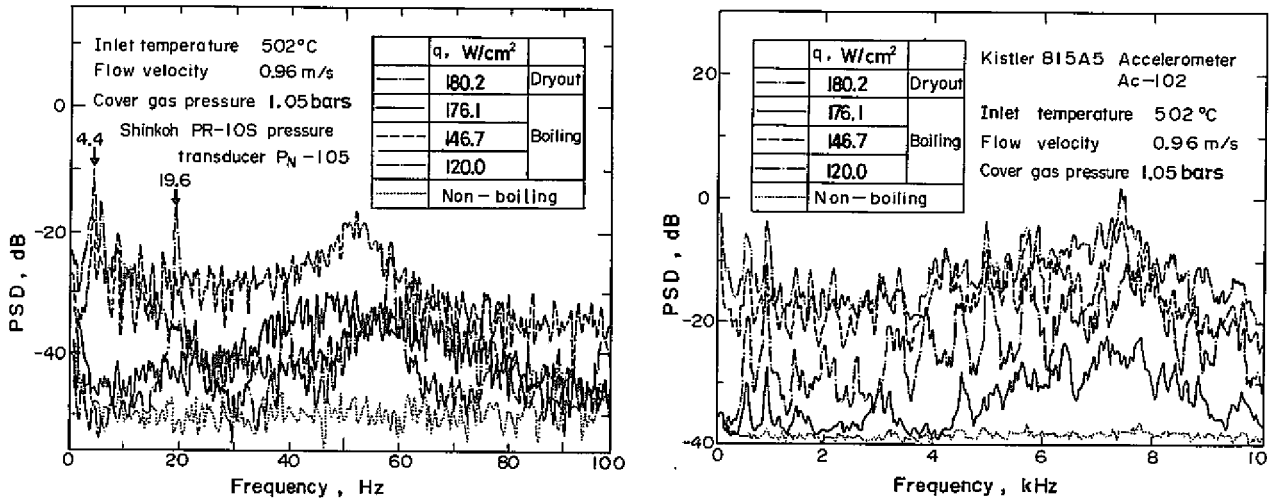

(a) Low frequency ranges　　(b) High frequency ranges

Fig. 6 Frequency spectra of acoustic noise with boiling in a locally blocked seven-pin bundle —— steady-state boiling run 7(6)LB-214

tion of the outlet flowmeter. In this state the flow fluctuation caused by the repetition of bubble formation and collapse increases with rising heat fluxes, since the liquid around the bubbles is yet so highly subcooled that the bubbles collapse completely although the bubbles become larger with higher heat fluxes.

The decreasing fluctuation intensity after the maximum can be attributed to the decrease in subcooling, which slows down the collapse of bubbles and so reduces the flow fluctuation.

The final fluctuation increase resulting from the rapid upstream voiding is due to the ejection of liquid films and/or liquid globules, then to the succeeding generation of a large amount of vapor bubbles.

Spectrum of Flow Fluctuation

Figure 8 shows the frequency spectra of outlet flow fluctuation during the same boiling run 7(6)LB-214. The peak observed at the frequency of 19.6 Hz for the heat flux of 120.0 W/cm^2, is due to the repetition of bubble formation and collapse. The peak at 4.4 Hz for 146.7 W/cm^2 is also due to the same process.

Bubble Size and Frequency

The bubble size and the frequency of bubble formation are important for the estimation of dryout in local boiling. But there are little data on sodium boiling. This led the present

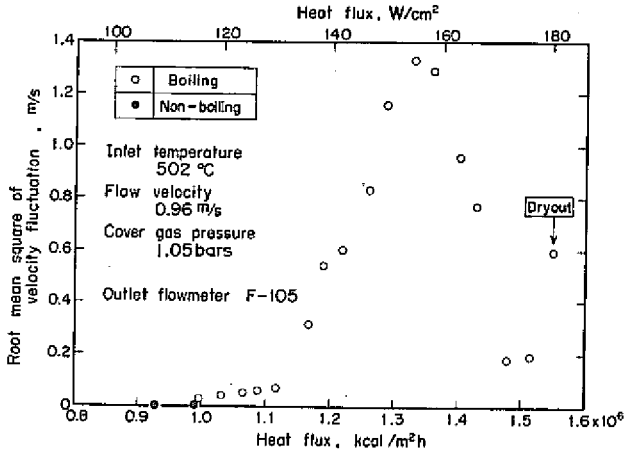

Fig. 7 Effect of heat flux on root mean square of outlet flow velocity fluctuation with boiling in a locally blocked seven-pin bundle —— steady-state boiling run 7(6)LB-214

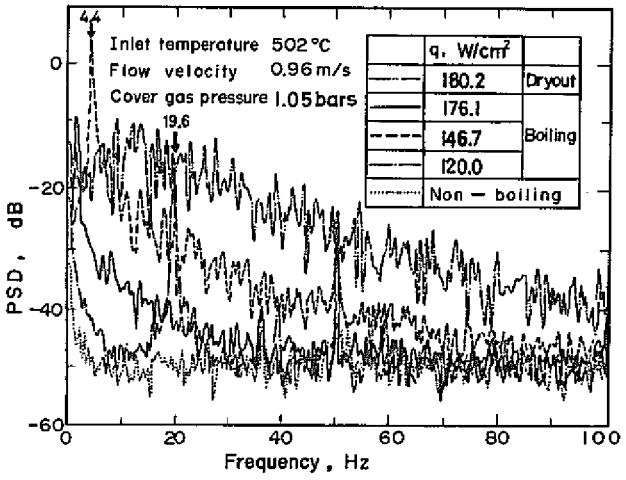

Fig. 8 Frequency spectra of outlet flow velocity fluctuation with boiling in a locally blocked seven-pin bundle —— steady-state boiling run 7(6)LB-214

authors to carry out a study on sodium to examine the bubble size and frequency in subcooled boiling under forced convection. In Fig. 9 the frequency, f is plotted against the diameter d_o of an equivalent sphere having the same volume as the bubble when it attained its maximum size. In this figure are also shown the earlier single-pin experiments[2] and the pool boiling experiments with potassium by Bobrovich et al.[6]

The sodium bubble is considerably larger than the water bubble, because of the high liquid-to-vapor density ratio of sodium. It is considered that the generation of a second bubble is inhibited by the pressure rise due to the development of the first bubble in the narrow space of the channel. This justisfies the assumption that only one bubble exists at one time, which permits evaluation of the frequency of bubble formation from the observed oscillations of the outlet flowmeter records during the period preceding the arrival of the bubbles to the flowmeter position. On the other hand, the volume of the bubble may be evaluated by integrating the increment of outlet flow rate between the instant of bubble formation and that of its attaining maximum volume.

From Fig. 9, it is seen that the frequency decreases with the increase of the bubble diameter, and that this diameter is a little influenced by flow velocity. A broken-line curve can be drawn, which roughly represents the relation between the diameter and the

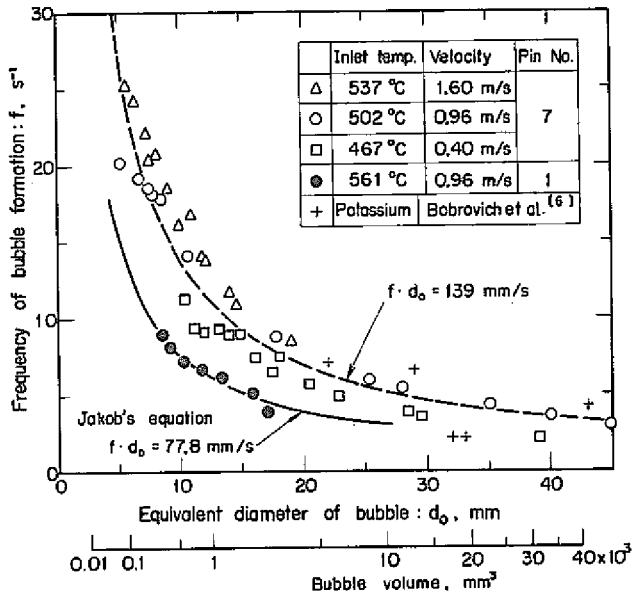

Fig. 9 Relation between equivalent diameter of bubble and frequency of bubble formation for sodium boiling

frequency in the present seven-pin experiment. This relationship is expressed by

$$f \cdot d_o = 139 \text{ mm/s } (=500 \text{ m/h}).$$

This product value is higher than that of $f \cdot d_o = 77.8$ mm/s (=280 m/h) obtained in the previous single-pin experiment, and agrees well with the pool boiling experiment for potassium by Bobrovich et al. This fact can be attributed to the two-dimensional bubble growth and collapse which was absent in the previous single-pin geometry. The bubble can expand and collapse not only in the axial direction, but also in the radial direction.

CONCLUSIONS

Experimental studies were carried out on local sodium boiling in the downstream of a local flow blockage in a seven-pin electrically heated LMFBR fuel subassembly mockup. In the first series of experiments the temperature distributions in the downstream of the blockage were measured under non-boiling conditions. In the second series of experiments, however, local boiling phenomena were investigated, with particular emphasis on the behavior of the two-phase flow pattern, the characteristics of boiling acoustic noise and outlet flow fluctuation, and the relation between the bubble size and the frequency of bubble formation.

Analyses of the results obtained permit the following conclusions to be drawn:

(1) In the non-boiling experiments the hottest surface temperature of the central pin was observed immediately downstream from the blockage. The measured temperature rise was in fairly good agreement with the calculation by the LOCK code. When the experimental results with the LOCK code are extrapolated to the prototype reactor conditions, namely the heat flux of 200 W/cm^2 and the flow velocity of 5 m/s, the temperature rise due to a central six-subchannel blockage will be less than 250°C.

(2) In the local boiling region, no flow instability was observed since the subchannels near the wrapper wall were still filled with subcooled liquid. The pressure drop appeared to remain constant. This is an important point to be borne in mind in reactor safety considerations, since local boiling of

sodium will not necessarily always bring about instability of flow. In the nearly bulk boiling region, however, considerable upstream voiding occurred and then the inlet flow decreased. The inlet flow reversal occurred and resulted in a final dryout.

(3) The boiling caused a considerable increase in acoustic noise intensity. The noise intensity with boiling first increased with rising heat fluxes, and after attaining a maximum, decreased somewhat to remain constant thereafter. Upon the final upstream voiding which resulted in the dryout condition, however, the noise intensity again increased sharply. The noise intensity of approximately 20 mbar in the RMS value obtained in the present sodium boiling experiment is much higher than that of approximately 0.5 mbar in the ordinary pool boiling experiments with water. The above observation indicates that the measurement of acoustic noise signals associated with sodium boiling phenomena is promising for early detection of local sodium boiling in LMFBR fuel subassemblies.

The peak observed at the low-frequency hertz ranges was due to the repetition of bubble formation and collapse. In the high-frequency kilohertz ranges, however, resonance peaks were superposed on a smooth curve with a broad peak at approximately 7 kHz.

(4) The boiling caused an increase in the outlet flow fluctuation, and the maximum RMS value of the flow fluctuation was 1.33 m/s. Therefore the measurement of outlet flow fluctuation signals appeared to be promising for early detection of local sodium boiling in LMFBR fuel subassemblies.

(5) The frequency of bubble formation ($2.9\ s^{-1}$ and $20.2\ s^{-1}$) decreased with the increase of the bubble size at its point of maximum development. The product of the bubble frequency and equivalent diameter obtained in the present seven-pin experiment agreed fairly well with the potassium pool boiling experiments by Bobrovich et al., and can be expressed in the relationship of $f \cdot d_o$ = 139 mm/s (=500 m/h), which is higher than that of $f \cdot d_o$ = 77.8 mm/s (=280 m/h) obtained in the previous single-pin experiment.

(6) Larger-scaled experiments both in 19-pin and 37-pin bundles are scheduled for this year and next, and the propagation of local boiling to bulk boiling will be investigated in detail, since the present seven-pin experiments were insufficient for this purpose.

ACKNOWLEDGMENTS

The authors wish to acknowledge the technical contributions of Mr. K. Haga, Mr. T. Okouchi and Mr. T. Komaba at all the stages of the experiments.

REFERENCES

1. Y. Kikuchi et al., "Loss-of-Flow Tests in Single- and Seven-Pin Geometries," ASME paper 74-WA/HT-44, New York (1974).
2. Y. Kikuchi et al., "Experimental Study of Steady-State Boiling of Sodium Flowing in a Single-Pin Annular Channel," J. Nucl. Sci. Technol., 12, 83 (1975).
3. M. Jakob, Heat Transfer, Vol.1, John Wiley & Sons Inc., New York (1958).
4. A. Ohtsubo, "Analytical Code LOCK on a Few Channels-Blockage Accident," PNC Rep. N251 74-32 (1974).
5. For instance, Y. Bessho, "Experimental Study of Acoustic Noise in Subcooled Nucleate Pool Boiling with Water," Master's Thesis, Kyoto University (1975) (in Japanese).
6. G. I. Bobrovich et al., "On the Mechanism of Boiling of Liquid Metals," Proc. JSME Semi-International Symposium Vol.2, Tokyo, Japan (1967) p.171.